Cavity-Enhanced Absorption Measurements Across Broad Absorbance and Reflectivity Ranges

ARTICLE *in* ANALYTICAL CHEMISTRY · APRIL 2014

Impact Factor: 5.64 · DOI: 10.1021/ac404251w

4 AUTHORS, INCLUDING:

Ruchika Bhawal
University of Texas at Arlington
7 PUBLICATIONS **7** CITATIONS
SEE PROFILE

Akif Ibragimov
Texas Tech University
109 PUBLICATIONS **332** CITATIONS
SEE PROFILE

analytical chemistry

Article

pubs.acs.org/ac

Cavity-Enhanced Absorption Measurements Across Broad Absorbance and Reflectivity Ranges

Purnendu K. Dasgupta,* Ruchika P. Bhawal, and Yin-Huan Li†

Department of Chemistry and Biochemistry, University of Texas at Arlington, Arlington, Texas 76019-0065, United States

Akif Ibraguimov

Department of Mathematics and Statistics, Texas Tech University, Lubbock, Texas 79409-1042, United States

Supporting Information

ABSTRACT: Cavity-enhanced spectrometry constitutes an important and highly sensitive technique for absorbance measurements. The current practice generally involves very high reflectivity mirrors and hence intense light sources (typically lasers) to have enough light transmitted. Available theory describes the situation only for high-finesse cavities (high-reflectance mirrors) and generally for systems with very low absorbances. We develop the general expression for absorbance regardless of mirror reflectivity or the absorbance and show that in the limit of high reflectivities and low absorbances it predicts the same numerical values as that derived by O'Keefe (*Chem. Phys. Lett.* **1998**, *293*, 331−336; *Chem. Phys. Lett.* **1999**, *307*, 343−349). Signal to noise in any photometric system is also dependent on the amount of light reaching the detector because of shot noise limitations. We show that a small aperture in the entrance mirror greatly improves light throughput without significant departure from the theoretically predicted amplification of absorbance; such simple modifications result in real improvement of detection limits, even with mirrors of modest reflectivity and inexpensive detectors. This allows the merits of cavity enhancement measurements to be demonstrated for pedagogic purposes.

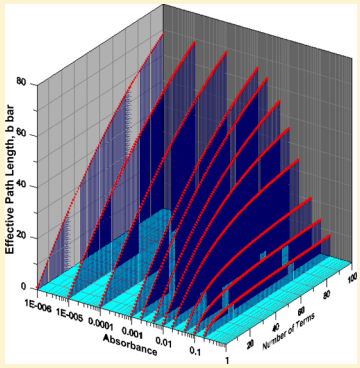

Absorption spectrometry is arguably the most commonly used quantitation technique used for analysis. To increase detection sensitivity, one chooses the optimum chemistry and the measurement wavelength (absorptivity ε at maximum). Absorbance also increases with the path length. In the gas phase, single long paths as in differential optical absorption spectroscopy[1] or one attained through multireflection cells[2,3] can be used. Simply increasing the absolute value of the absorbance is not tantamount to improving the limit of detection (LOD), however. In the liquid phase, due to increased beam divergence, light is rapidly lost to the wall and noise increases rapidly as the detector is light-starved. Thin-walled straight glass tubes[4] or those filled with high refractive index (RI) organic solvents[5,6] help guide light via total internal reflections at the glass−air and solvent−glass interfaces, respectively; neither system is particularly useful. A gas shell can be formed around a liquid in a hydrophobic porous membrane tube,[7] but a gas bubble is too readily formed. Aqueous solutions containing a lot of solute or ethanol can have an RI greater than that of FEP Teflon 1.34 (RI 1.34), and thus an FEP tube filled with such a solution also behaves as a liquid core waveguide (LCW).[7,8] LCWs with purely aqueous solution as the core have become practical only after the introduction of Teflon AF (RI 1.29−1.31, compared to 1.33 for water).[9−11]

In all the above arrangements, the incident light assumedly traces a single path; these are both single-path and single-pass cells, i.e., the light does not trace the same path twice. Such cells have a single effective overall path length for the purposes of Lambert−Beer's law regardless of the cell contents. If a particular chemistry−wavelength combination leads to a certain dynamic range, changing the path length will merely change the location of the usable range in the concentration domain.

In contrast, a multipath arrangement behaves differently: If the shortest path that the light can travel to reach the detector is b, the effective path length (henceforth designated $\overline{b}$) is absorbance-dependent. It is readily perceived that, at high absorbances, longer paths contributes little to the transmitted light and $\lim_{A=\infty} \overline{b} = b$. The value of $\overline{b}$ at the lower absorbance limit is often the determinant of the concentration LOD. For a multiplicity of pathlengths b_i, each having f_i fraction of the total light ($\Sigma f_i = 1$), it has been shown that $\overline{b}$ at the lower absorbance limit is simply the weighted sum $\Sigma f_i b_i$.[12] For an evenly illuminated wedge-shaped cell,[13,14] for example, at the lower absorbance limit $\overline{b}$ will be half the base width of the cell.

The combination of cells with different pathlengths is not practical; moreover, $\lim_{A=0} \overline{b}$ will still be less than the longest physical path length. Putting partially reflective mirrors on both entrance and exit windows of any conventional cell serves the same purpose.[15] In the following we consider such a system as a

Received: June 20, 2013
Accepted: March 19, 2014
Published: March 19, 2014

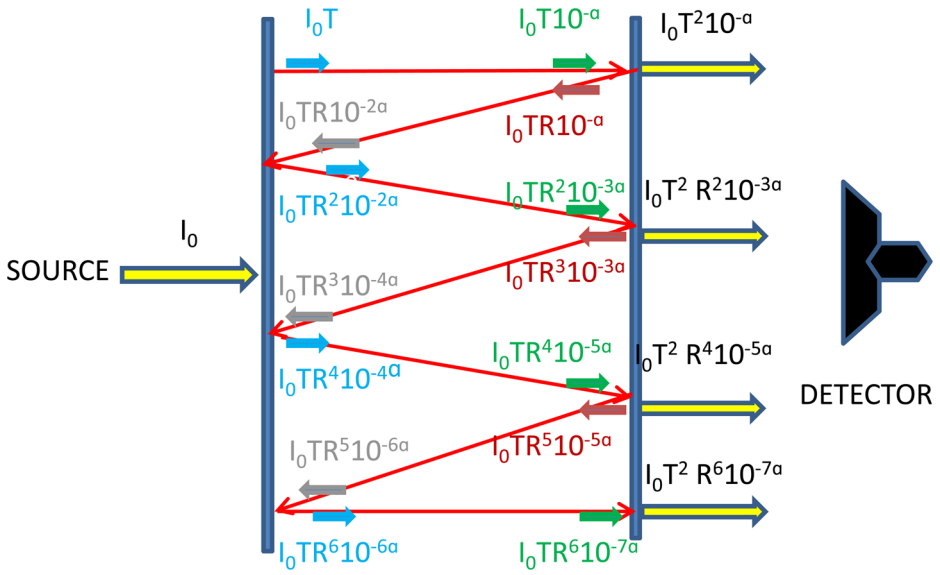

Figure 1. Single-path multipass cell arrangement, schematically shown. The individual ray traces are all actually perpendicular to the mirrors and are superimposed on each other. They are shown in this manner to indicate the intensity after each event. Similarly, a single beam emerges to fall on the detector. Mirror reflectance is R, transmittance is T, extinction coefficient of the medium is α.

single-path multipass cell (multiple reflections on the same path as the beam traverses back and forth, each time losing light both due to absorption by the medium and transmission through the partially transmissive windows).

PRINCIPLES

Optics and the analytical chemistry literature, respectively, use natural and base-10 logarithmic relationships to describe light extinction. We will denote the respective extinction coefficients as α' and α [$\alpha' = \alpha \ln(10)$], the base-10 version of Lambert's law being $I = I_0 10^{-\alpha b}$, where I_0 and I are the total incident and transmitted light intensities, and α is equal to εc, ε being the molar absorptivity of the solute and c its concentration. We assume the base path length b, on each side of which a partial mirror is placed, to be unity. Since units are not specified, any conclusion will be equally valid for any other value of b. With $b = 1$, $\bar{b}$ is not only the effective path length, it is also the amplification factor of the physical path length, sometimes referred to as the cavity enhancement factor.[16,17] We denote the reflectance and the transmittance of the mirror as R and T, respectively, and assume that $R + T = 1$, i.e., mirror absorptance is negligible (note, however, that it can readily be shown that a finite absorptance has no effect on the results, except for a reduction in the overall light throughput).

Although Fielder et al.[18,19] have more recently considered the theoretical aspects of single-path multipass systems, the focus is on the accurate determination of α. We provide below an accurate mathematical description that adequately takes into account finite absorption by the intervening medium.

Figure 1 depicts a partially reflective mirror each placed on each side of the measurement cell. Following notations used above, with I_0 incident on the entrance mirror, I_0T enters the cell. Light reaching the exit mirror is $I_0T10^{-\alpha}$ of which $I_0T^210^{-\alpha}$ is transmitted and $I_0TR10^{-\alpha}$ is reflected. Light is again attenuated as it traverses the cell and reaches the entrance mirror with the intensity $I_0TR10^{-2\alpha}$. $I_0TR^210^{-2\alpha}$ is reflected back, $I_0TR^210^{-3\alpha}$ reaches the exit mirror, and $I_0T^2R^210^{-3\alpha}$ is transmitted. The total transmitted light I is represented by the infinite geometric series:

$$I = I_0T^210^{-\alpha}\sum(1 + r + r^2 + r^3 + r^4 + ...) \quad (1)$$

where $r = R^210^{-2\alpha}$.

Recognizing that the sum of the geometric series in parentheses is $(1 - r)^{-1}$, eq 1 reduces to

$$I = \frac{I_0T^210^{-\alpha}}{(1 - R^210^{-2\alpha})} \quad (2)$$

This leads to the expression of $\bar{b}$ (see the Supporting Information):

$$\bar{b} = \frac{1}{\alpha}\log\left(\frac{1 - R^210^{-2\alpha}}{10^{-\alpha}(1 - R^2)}\right) \quad (3)$$

Note that in deriving eq 3, there was no implicit assumption that mirror absorptance is negligible or that the reflectivity is necessarily very high; it is valid for values of R or $R + T$ significantly less than 1. At the low-absorbance limit of eq 3, it is readily derived (see the Supporting Information):

$$\lim_{\alpha\to 0}\bar{b} = \frac{1 + R^2}{1 - R^2} \quad (4)$$

The same system has previously been considered by Dasgupta and Rhee[15] and O'Keefe.[20,21] The former used an interferometric model—such a model will be inapplicable here as the bandwidth of the source and the quality of the cavity will not be expected to hold in the present experiments. In any case, a comparison with the limits from the interferometric predictions[15] with the above model is given in the Supporting Information. O'Keefe assumed negligible mirror absorptance and derived (we have taken the liberty to correct a missing minus sign)

$$I = -\frac{I_0T^2e^{-\alpha'}}{2\ln(Re^{-\alpha'})} \quad (5)$$

O'Keefe did not explicitly calculate the gain in path length, but this can be readily computed from eq 5 (see the Supporting Information) to be

dx.doi.org/10.1021/ac404251w | Anal. Chem. 2014, 86, 3727−3734

$$\bar{b} = \frac{1}{\alpha'}\ln\left(\frac{\ln(R) - \alpha'}{e^{-\alpha'}\ln(R)}\right) \quad (6)$$

At the low-absorbance limit

$$\lim_{a'\to 0} \bar{b} = 1 - \frac{1}{\ln(R)} \quad (7)$$

A comparison of eqs 3 and 6 for $\bar{b}$ as a function of α for various values of R appears in Figure 2. The figure is in logarithmic scale

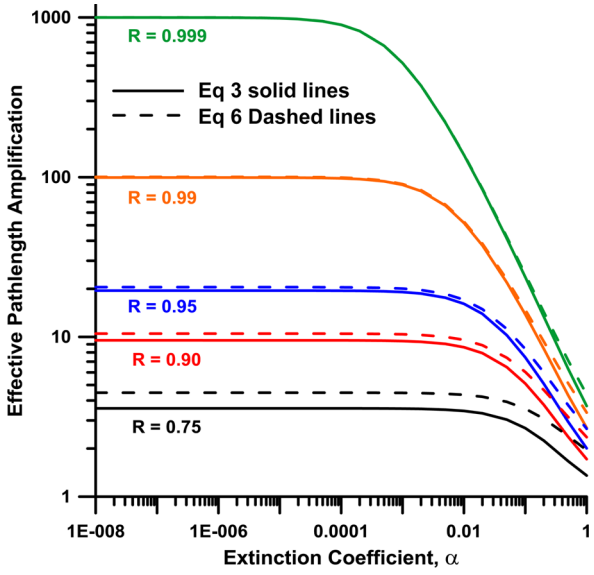

Figure 2. Difference between the geometric series summation (eq 3) and the O'Keefe approaches (eq 6) in predicting $\bar{b}$ as a function of α for various values of R.

to cover a large span; unfortunately, such scaling also minimizes the visual difference. Nevertheless, it is apparent that the expectations from both equations are nearly the same at high values of R and low values of α and there is significant difference when either R is low or α is high. It may also be noted that, for either eq 3 or 6, at high values of R, the limiting value of $\bar{b}$ is approximately given by

$$\lim_{R\to 1,\alpha\to 0} \bar{b} \cong \frac{1}{1 - R} \quad (8)$$

Table S1 in the Supporting Information shows the $\lim_{R\to 1,\alpha\to 0}$ values according to eqs 4, 7, and 8. It is interesting to note that at high R, eqs 4 and 7 approach the value predicted by eq 8 but from opposite directions.

When Only a Finite Number of Reflections Count. Even in a nominally single-path multipass system of perpendicular beam incidence, there is finite beam divergence and a finite detector area. All of the light coming out on the detector side cannot possibly be captured by the detector. Thus, a real situation likely represents a finite number of reflections. This is easily simulated by truncating the infinite series expression in eq 1 to any desired number of terms. The results for 1−100 terms summed for a standard 1 cm path cell, for absorbance values ranging from 10^{-6} to 0.2, are shown in Figure 3 for mirrors with R = 0.99. Note that "number of terms" is not synonymous with number of passes counted. When we count three terms, for example, the first term results from a single base path traverse, while the second and the third terms result from three and five base-path traverses, respectively.

As may be intuitive (if we limit ourselves to a single term, that is, standard Beer's law behavior; $\bar{b}$ can be >1 only in the presence of subsequent terms), $\bar{b}$ increases with increasing number of terms summed (Figure 3), although, even after 100 terms, it does not reach the limit predicted by eq 4 (compare Figure 3a vs Figure 2) R = 0.99 traces. Given the same number of terms, $\bar{b}$ also increases with decreasing α (Figure 3b), much the same as the infinite series sum in Figure 2, except that the sum obtained here is less than that from eq 3. In the above considerations, we have assumed that the number of terms that count and the extinction coefficient α are independent variables. In reality, when light loss in each pass is significant, e.g., because beam divergence is high or

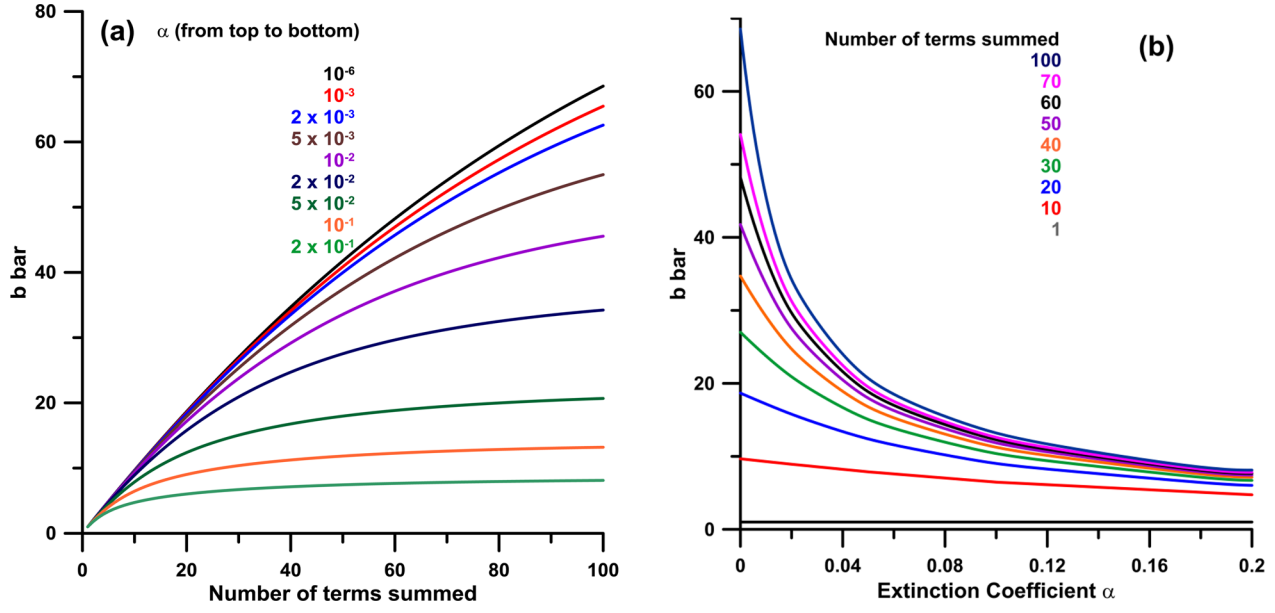

Figure 3. Effect of finite number of reflection terms summed in eq 7 for different values of the extinction coefficient α on the effective path length $\bar{b}$. If panel b is plotted with a logarithmic abscissa, qualitatively it will have the same shape as Figures 2 and 4.

dx.doi.org/10.1021/ac404251w | Anal. Chem. 2014, 86, 3727−3734

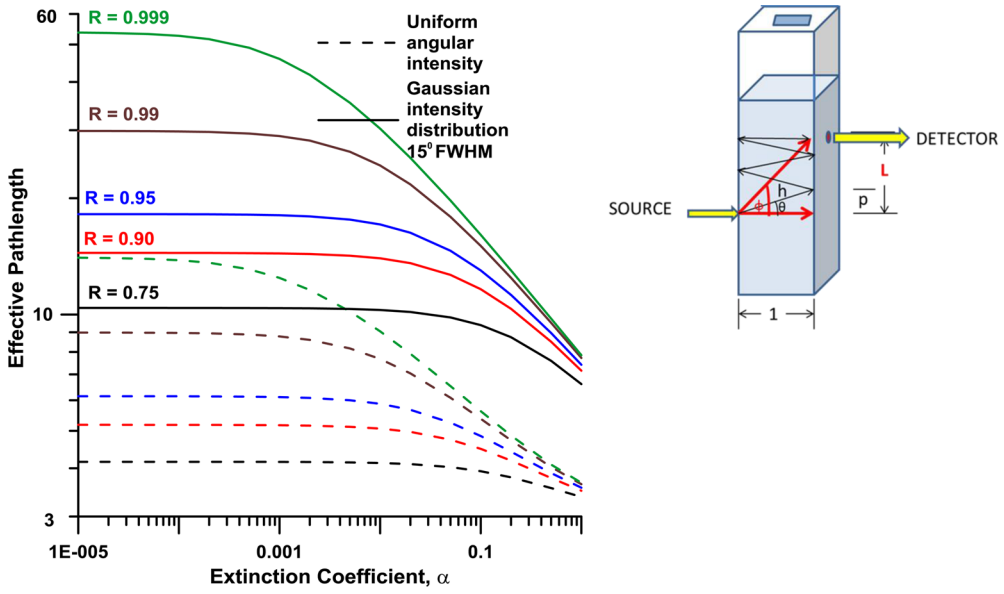

Figure 4. Effective pathlengths computed for the cell arrangement in the inset. In this off-axis arrangement, both entrance and exit apertures are present to increase light throughput. The entrance and exit sides act as reflective mirrors. L is the vertical distance between the entrance and exit point, Φ is the angle between the vertical distance "L" and the shortest path length (considered as unity for standard cells), θ is the angle between the vertical distance "p" and the shortest path length, and "h" is the distance traveled by the incident light at an angle θ. Note logarithmic axes in the plot. Note that the shortest source detector distance is $\sqrt{2}$, if this is considered the base path length; the path length amplification factor is ~40% less than the ordinate values shown.

R is low, the effective number of terms will decrease with increasing α.

Ultimate Limitations: Why the Source Must Provide Enough Power. Light throughput is a most important consideration. In an ideal situation the system must operate in the detector shot-noise-limited domain. If there are temporal source fluctuations, it is assumed that this can be compensated for by referencing. If light reaching the detector is not sufficient, whether because R is too high or I_0 is too low for the detector to operate in the shot-noise-limited domain, increasing the absorbance signal will not result in any improvement in lowering the LOD, which is typically defined on the basis of S/N = 3. Putting mirrors of very high R on each side of a cuvette in a standard spectrophotometer will deteriorate the LOD, not improve it.

The signal S in the present case is the difference in the amount of light reaching the detector in the presence of an absorbing sample ($\alpha = \alpha$) from that when $\alpha = 0$. Adapting eq 2

$$S = I_{a=0} - I_{\alpha=\alpha} = \frac{I_0T^2}{(1-R^2)} - \frac{I_0T^2 10^{-\alpha}}{(1-R^2 10^{-2\alpha})} \tag{9}$$

Assuming zero absorptance ($R + T = 1$) eq 9 reduces to (see the Supporting Information)

$$S = \frac{I_0(1-R)\alpha'(1+R^2)}{(1+R)(1-R^2(1-2\alpha'))} \tag{10}$$

Only for R approaching unity, at low values of α, eq 10 will further reduce to

$$S = \frac{I_0\alpha'}{2} \tag{11}$$

On the other hand in a shot-noise-limited situation, the noise associated with each of the terms in eq 9 is proportional to the square root of each of the terms. As the noise will add in a root-mean-square fashion we can write the expression of the overall noise N as

$$N = k\sqrt{\left(\frac{I_0(1-R)^2}{(1-R^2)} - \frac{I_0(1-R)^2 10^{-\alpha}}{(1-R^2 10^{-2\alpha})}\right)} \tag{12}$$

where k is a constant of proportionality. This simplifies to (see the Supporting Information)

$$N = k\sqrt{\left(\frac{1+(1-\alpha')(1-2R^2)}{(1+R)(1-R^2(1-2\alpha'))}\right)} \tag{13}$$

Only for R approaching unity, at low values of α, eq 13 will further reduce to

$$N = k\sqrt{I_0(1-R)} \tag{14}$$

leading to the following expressions for S/N and LOD:

$$\mathrm{S/N} = 0.5\frac{\alpha'\sqrt{I_0}}{k(1-R)} \tag{15}$$

$$\mathrm{LOD} = 1.5\frac{\alpha'\sqrt{I_0}}{k(1-R)} \tag{16}$$

Nonlinear Amplification in a Multipath Configuration. The above considerations apply strictly for an incident light beam repeatedly traversing the same path. Effects of beam etendue/divergence or the dependence of the exact reflectance of high-R dielectric mirrors on the incidence angle are not accounted for. Even for a coherent/collimated beam, some beam divergence is likely upon a large number of reflections. There are several recent papers on cavity absorption experiments in liquids and/or with light-emitting diode (LED) sources, where source light may reach the detector via multiple paths. There have been no

dx.doi.org/10.1021/ac404251w | Anal. Chem. 2014, 86, 3727−3734

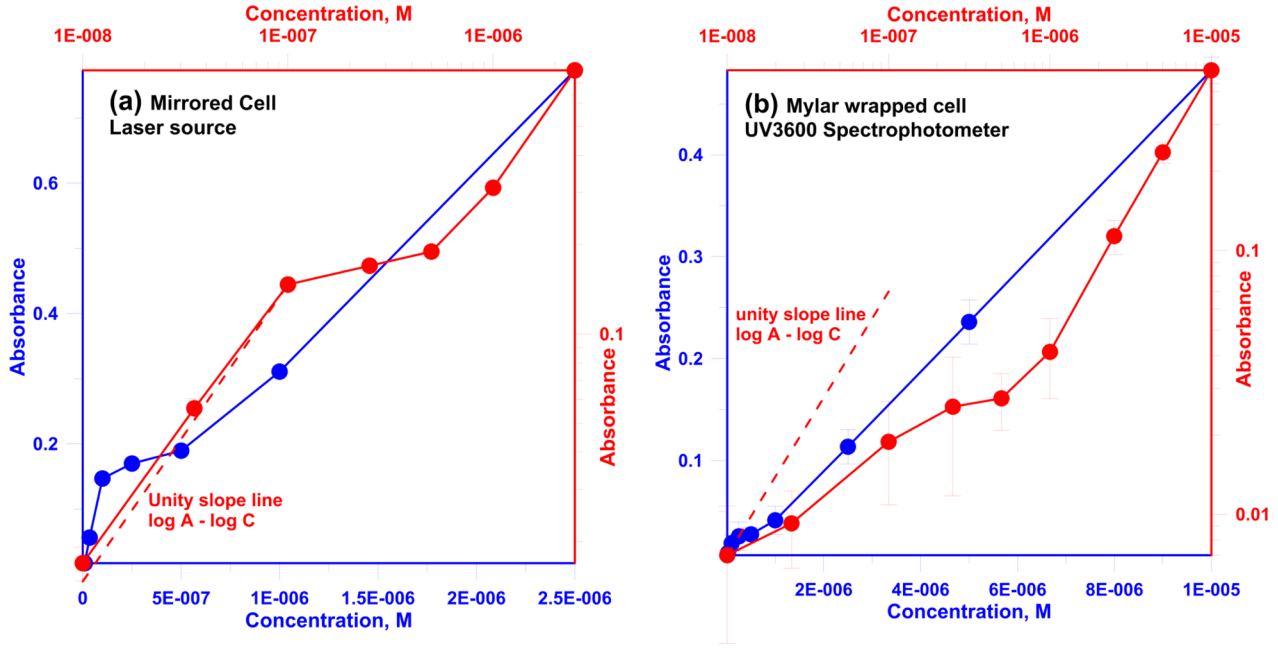

Figure 5. Beer's law behavior of bromocresol green at pH 12 in conventional linear as well as logarithmic axes. (a) Silver-mirrored cell (type 2) with a 633 nm laser and a CCD array detector. (b) Reflective Mylar-wrapped cell with the UV 3600 spectrophotometer as the source (617 nm, 2 nm slit width) and detector.

theoretical considerations of multiple paths originating from reflections within an enclosure.

When a divergent source is used, it would be of advantageous to introduce the light through a pinhole in the entrance mirror upon the first reflection and return; the light lost through the pinhole will be small compared to the total beam area. The overall light throughput will increase, however, by the factor $(1 - R_{entrance})^{-1}$. Consider the two-dimensional depiction of an externally silvered cuvette such that each wall behaves as a mirror, as depicted in the inset of Figure 4. A divergent source, e.g., a light-emitting diode (LED), is used to bring light through an aperture as indicated. The detector views the cell on the opposite side but located at a higher horizontal plane relative to the source, such that a direct ray traveling from the source to the detector will be at an angle ϕ relative to the horizontal. For convenience, we will assume that ϕ is $\pi/4$ rad, such that the source−detector vertical distance is the same as the horizontal base path b that we assume to be unity. The detector can be behind the exit mirror or behind a small exit aperture: again, as long as the detector size is small relative to the beam dimensions the theoretical considerations will differ little other than an increase in the light throughput by the factor $(1 - R_{exit})^{-1}$. We assume here the presence of an exit aperture. Light can also travel by reflection being incident at some other angle θ $(0 < \theta < \phi)$, and in doing so, the ray traverses a distance h, covering a vertical distance of p (equal to tan θ), as indicated. To reach the detector with a vertical rise of unity, these steps should occur n times where $n = 1/p$. The n steps result in a total beam traverse of $2hn$; in the process, $2n - 1$ reflections take place. Note also that hn is equal to $1/\sin\theta$. If $I_{0,\theta}$ is the initial intensity of the beam traveling with the angle θ, the transmitted light intensity I_θ will be given by

$$I_\theta = I_{0,\theta} R^{2n-1} 10^{-2hn\alpha} \tag{17}$$

The total transmitted light intensity I is then obtained by integration over $\theta_{0\to\phi}$:

$$I = \int_0^\phi I_{0,\theta} R^{((2/\tan\theta)-1)} 10^{-(2\alpha/\sin\theta)}\, d\theta \tag{18}$$

For $\phi = \pi/4$ rad (45°), we integrate eq 18 numerically as a function of α, with a resolution of 0.56 mrad (0.1°), for various values of R, and the results are shown as dashed line traces in Figure 3. These calculations assume that the initial intensity is the same at all angles; this of course is not the case for a real LED. If we assume the angular light intensity distribution of the LED is Gaussian and has a full width half-maximum (fwhm) of 0.26 rad (15°), $\bar{b}$ is much higher because the total light throughput shifts to a higher average traversed path length. The overall limiting $\bar{b}$ is, nevertheless, much less than what is expected in a single-path multipass paradigm as embodied in eq 3.

EXPERIMENTAL SECTION

We conducted experiments with two types of detection arrangements and disposable polystyrene cuvettes in three designs. The detection instruments ranged from a high-end commercial double-beam double-monochromator spectrometer capable of reading ±6.000 absorbance (http://www.shimadzu.com/an/spectro/uv/uv3600.html), to an inexpensive fiber-optic 12-bit CCD spectrometer (http://oceanoptics.com/products/usb2000.asp, now obsolete). The spectrophotometer measurements were made at the absorption maximum, with a slit width of 2 nm, except as stated. An identically prepared cell filled with water was used as the reference. With the CCD spectrometer, LEDs (center wavelengths of 617 and 522 nm) were used as the light source, generally just glued on the cell; the drive current was 50 mA. The detector integration time was typically 1.5 s. The same experiment was repeated using a 633 nm laser as the source.

The following were the cell designs: (1) The cell was wrapped with a single layer of reflective aluminized Mylar film (0.125 mm thick, sold as disposable emergency thermal blanket, www.sears.com). An aperture was made on the light entrance side of the cell positioned at the incident beam spot center (for the

dx.doi.org/10.1021/ac404251w | Anal. Chem. 2014, 86, 3727−3734

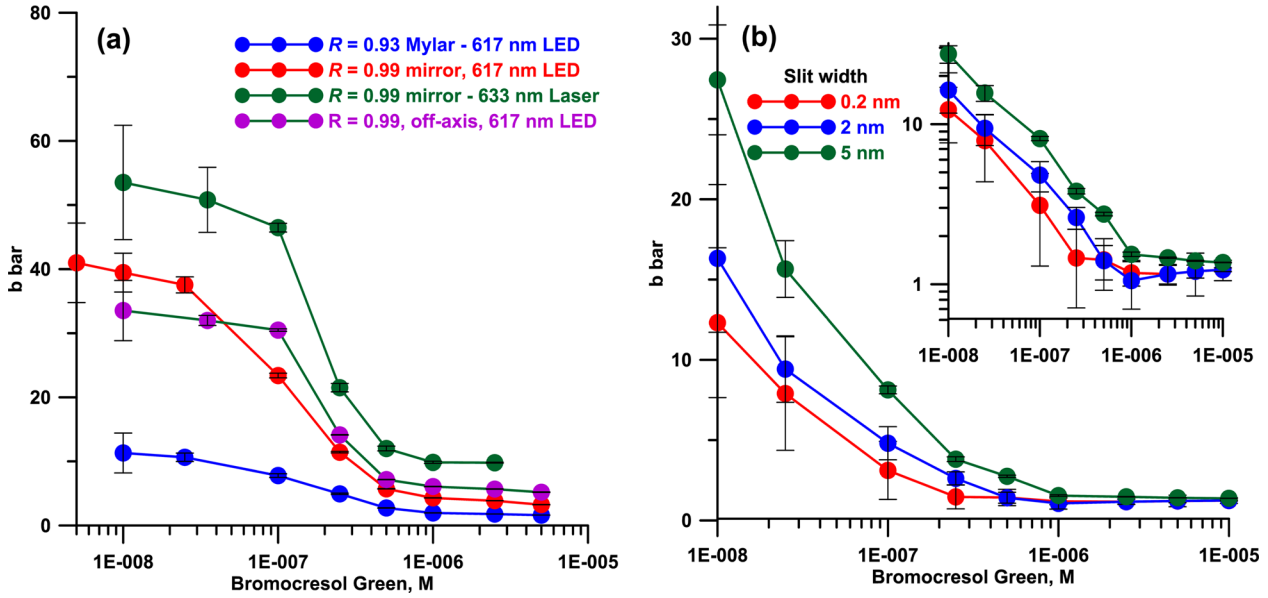

Figure 6. Experimental values of $\bar{b}$ as a function of bromocresol green concentrations with different cell types and (a) CCD spectrometer detector, (b) UV 3600 spectrophotometer detector, R = 0.99 mirrors. Inset shows the same data but with the ordinate on a logarithmic scale.

spectrophotometer, a rectangular 1 × 1.5 mm ($w \times h$), for the fiber-optic CCD a 0.8 mm diameter cutout). (2) Microscope slides were mirrored using a commercial silvering solution (www.peacocklabs.com); these were affixed on the light entrance and exit sides of the cell. For details of silvering, see the Supporting Information. By etching with HNO_3, an ∼0.5 mm aperture was made on the entrance mirror; the incident beam was directed through this aperture. The more reflective glass sides faced the cuvette; the exposed silver metal sides were protected with a thin layer of transparent optical grade epoxy. (3) The cell was essentially identical to that in type 2 except that the detector optical fiber was at a horizontal plane 1.8 cm higher relative to the source aperture (vertically offset, cf., Figure 4; this arrangement is hereinafter referred to as off-axis). Also in this case, light was read through a 0.5 mm aperture in the exit-side mirror, unlike type 2, where light was read through the mirror itself, without an aperture.

To make performance comparisons with and without reflective elements, the same type of cells, without any reflective elements, was used. To calculate effective path lengths ($\bar{b}$), the observed absorbance in the reflective cells is divided by the observed absorbance in the standard transparent cells. However, because the latter value was not directly measurable at very low concentrations, it was obtained by making Beer's law plots for each test dye (bromocresol green, bromothymol blue, and erythrosine B (FD&C red no. 3) in the 0.010−1.000 absorbance range, respectively, at 617, 615, and 522 nm. The first two were prepared in 1 mM NaOH; this was also used as the reference solution. Erythrosine B was prepared in water. Standard laboratory reagents were used. Diluted standards were typically prepared immediately before use, at the lowest concentrations, often in the measurement cell itself to prevent adsorption losses.

The Y-intercepts in the above Beer's law plots were statistically indistinguishable from zero, the linear relationship was excellent ($r^2 \geq 0.999$), and the molar absorptivities (ε) calculated from the slope were in excellent agreement with literature values. The absorbance in the conventional cell expected for the dye at the low concentrations was then computed from ε.

Reflectivities were measured typically at two wavelengths, using 633 nm (He−Ne), and 532 nm (frequency-doubled Nd:YAG) lasers, and a laser power meter (www.sperdirect.com).

Cell types 1 and 2 were examined with both the spectrophotometer and the CCD spectrometer; cell type 3 was examined only with the latter.

RESULTS AND DISCUSSION

Concentration−Apparent Absorbance Relationships. Figure 5 shows Beer's law behavior of bromocresol green at pH 12 in conventional linear as well as logarithmic axes. The beginning and ending values of both axes were the same such that the starting and the ending points in both the linear and logarithmic plots are coincident. Two representative cases are shown: (a) in a silver-mirrored cell (type 2) with a 633 nm laser and a CCD array detector and (b) a reflective Mylar-wrapped cell with the UV 3600 spectrophotometer as the source (617 nm, 2 nm slit width) and detector. In Figure 5a, referring to the linear axes there are three distinct regions: (i) a very steep A versus C linear relationship at the low concentration end, (ii) a less steep linear portion at the higher concentration end, and (iii) a transition region of low slope in between. The ratio of the two slopes in regions i and ii is the plateau value of the path length amplification factor in Figure 2, and the plateau is attained in region i. The same three regions are also observed in the log−log plot; the noteworthy item is that log A−log C slope is very close to unity in both regions i and ii. We refer to this as type A behavior, in which plateau value is reached. Figure 5b shows the other type of behavior: while this also exhibits three regions and the log A−log C relationship has a unit slope at the higher concentration end, the log A−log C slope is significantly less than unity at the lower concentration end. In this type of behavior (hereinafter called type B) a plateau of path length amplification factor is not observed; this will become more apparent in the next section. The data in Figure 5b also clearly show a greater standard deviation relative to that in Figure 5a because of poor light throughput resulting from a broad-band source and a narrow slit width. An increased slit width increases light throughput and reduces the standard deviation of the measurements (it also

dx.doi.org/10.1021/ac404251w | Anal. Chem. 2014, 86, 3727−3734

Table 1. Summary of Results, CCD Spectrometer Detector

cell type	analyte	reflectivity	lowest tested concn, nM[a]	effective path length at lowest concn, $\bar{b}$ cm	LOD_1, nM[b]	LOD_2, nM[c]
conventional, no mirror	bromocresol green, ε = 39100 M^{-1} cm^{-1}	NA		1	36	
type 1: reflective Mylar, entrance aperture, 617 nm LED	bromocresol green	0.93 at 633 nm	10	11 ± 0.5	8	8
type 2: glass mirror, entrance aperture, 617 nm LED	bromocresol green	0.99 at 633 nm	10	41 ± 3.2	4	4
type 2: 633 nm laser source	bromocresol green	0.99 at 633 nm	10	55 ± 16	3	3
type 3: off-axis 617 nm LED	bromocresol green	0.99 at 633 nm	10	33 ± 4.7	12	9
conventional, no mirror	erythrosine ε = 87500 M^{-1} cm^{-1}	NA	25	1	46	
type 1: reflective Mylar, entrance aperture, 522 nm LED[d]	erythrosine	0.89 at 532 nm	25	8.2 ± 0.8	5	4
type 2: glass mirror, entrance aperture, 522 nm LED[d]	erythrosine	0.91 at 532 nm	25	8.8 ± 0.3	4	0.4

[a]Lowest concentration measured; not considered if below the LOD. [b]Based on the terminal slope of the absorbance vs concentration curve. [c]Based on the terminal slope of the log(absorbance) vs log(concentration) curve. [d]At low concentrations, log A varies linearly with log C.

Table 2. Summary of Results, UV Spectrophotometer Detector[a]

cell type	analyte	reflectivity	lowest tested concn, nM[b]	effective path length at lowest concn, $\bar{b}$	LOD_1, nM[c]	LOD_2, nM[d]
conventional, no mirror	bromocresol green at 617 nm				47	
type 1: reflective Mylar, entrance aperture	bromocresol green at 617 nm	0.93 at 633 nm	10	16 ± 4.6	33	5
type 2: glass mirror, entrance aperture	bromocresol green at 617 nm	0.99 at 633 nm	25	95 ± 23	6	0.4
conventional, no mirror	erythrosine at 522 nm				13	
type 1: reflective Mylar, entrance aperture	erythrosine at 522 nm	0.89 at 532 nm	12.5	26 ± 4.3	8	7.3
type 2: glass mirror, entrance aperture	erythrosine at 522 nm	0.91 at 532 nm	12.5	48 ± 12	10	7.2

[a]At low concentrations, there is no linear relationship between A and C, log A varies linearly with log C in all of these experiments. [b]Lowest concentration measured; not considered if below the LOD. [c]Based on the terminal slope of the absorbance vs concentration curve. [d]Based on the terminal slope of the log(absorbance) vs log(concentration) curve.

increases the effective path length amplification factor); all LOD data for the spectrophotometric measurements are therefore reported for measurements made with a 20 nm slit width.

The Limiting Value of $\bar{b}$. Type A behavior was observed in all experiments with the laser or narrow-angle LED sources; the results were in accordance with the theoretical expectations depicted in Figures 2, 3b, and 4b. Namely, a limiting plateau value of $\bar{b}$ was attained or approached (Figure 6a). The observed $\lim_{\alpha\to 0}\bar{b}$ value was also well-predicted by theory. For example, in the laser source experiment (green trace, Figure 6a) the $\lim_{\alpha\to 0}\bar{b}$ was ∼55, which would be expected for mirrors with R = 0.982; the measured R was 0.99 ± 0.01. The identical experiment, except with a more divergent LED source, will be expected to have a lower limiting $\bar{b}$ because of earlier series truncation; $\lim_{\alpha\to 0}\bar{b}$ in this case (red trace, Figure 6a) was ∼40. For a 15° fwhm LED, we calculate for the R = 0.99 case a $\lim_{\alpha\to 0}\bar{b}$ of 30 (Figure 4); the experimental $\lim_{\alpha\to 0}\bar{b}$ value was ∼35. For R = 0.93, $\lim_{\alpha\to 0}\bar{b}$ is expected to be 13.8 (eq 4); the observed value at the lowest measured concentration was 11.3 ± 3.1.

Type B behavior was observed in all spectrophotometer experiments as well as with the CCD detector when used in combination with divergent sources, e.g., wide viewing angle LEDs. As shown in Figure 6b, in type B behavior, there is no indication that a limiting plateau value of $\bar{b}$ is being approached. Rather, $\bar{b}$ increased exponentially with decreasing log(concentration), within the lower limits of the analyte concentrations that could be reliably measured, as shown in Figure 6b. Increasing spectrophotometer slit width increases beam divergence, and as Figure 6b shows, the observed effect is more pronounced. Although we have not formulated a quantitative relationship, it is intuitive that this behavior will be expected; effectively, the number of terms that matter in a truncated series increases with decreasing α. For similar reasons (because extinction is more rapid) in entrance aperture based cells (admitted light intensity is not dependent on mirror reflectivity) the number of terms effectively decreases with decreasing mirror reflectivity. The observed absorbance (directly proportional to $\bar{b}$)−concentration relationship will obviously be different in type A versus type B behavior. When type A behavior is followed and a plateau value of $\bar{b}$ has been reached, then absorbance is directly proportional to concentration, and this value of $\bar{b}$ is synonymous with the term "cavity enhancement factor", and Lambert−Beer's law will be followed in the $\bar{b}$ plateau region. On the other hand, when $\bar{b}$ increases exponentially with decreasing concentration, it is obvious that Lambert−Beer's law is *not* followed. As a first approximation, log A or (log $\bar{b}$) is linearly related to log C in this regime, as shown in the inset of Figure 6b. Of course, in type A behavior, when A is linearly related to C with a near-zero intercept, log A is also linearly

dx.doi.org/10.1021/ac404251w | Anal. Chem. 2014, 86, 3727−3734

related to log C. In contrast, in type B behavior, A is not necessarily linearly related to C.

Limits of Detection. As previously stated, increasing the absorbance has no practical value unless there is actual gain in the limit of detection (LOD). Tables 1 and 2 list the observed experimental data for the CCD spectrometer and the spectrophotometer, respectively, that demonstrate that real improvements in LODs are achieved.

The LODs were calculated by two different methods. One assumed a linear relationship between A and C, and the other assumed a linear relationship between log A and log C. The absorbance of the blank was measured 5 times, and the LOD was taken to be the C value corresponding to 3 times the standard deviation of the blank on the A versus C or log A versus log C plot, respectively. The two calculated LOD values differed significantly only with systems displaying type B behavior, when A is not linearly related to C; in these cases the logarithmic relationship based LOD will be more appropriate. For comparison, measurements were also made in a conventional (no mirrors) cell. The linear relationship between A and C was confirmed in the absence of mirrors, and the LOD was computed from slope of the terminal two points above the LOD and 3 times the uncertainty of the blank as indicated above. In all cases the LOD improved in the cavity-enhanced measurements, in some cases by more than an order of magnitude.

In summary, we have provided a generally applicable (regardless of the exact values of R, T, or α), mathematical foundation for cavity-enhanced absorption measurements and introduced the concept of an input aperture for the cavity. This is of value in any situation where beam divergence is significant. An entrance aperture results in much greater light throughput without significant loss of cavity enhancement and thus reduces the need for increased source brightness for sufficient light to reach the detector for shot-noise-limited operation. This should provide an attractive means to make sensitive absorbance measurements with good light throughput in systems where the physical path length is very limited, e.g., in capillary systems. We also show that similar nonlinear absorbance amplification can result from the multipath effect in a reflecting cavity that contains an entrance and additionally an optional exit aperture that do not necessarily directly face each other.

■ ASSOCIATED CONTENT

Supporting Information

Additional information as noted in text. This material is available free of charge via the Internet at http://pubs.acs.org.

■ AUTHOR INFORMATION

Corresponding Author

*E-mail: dasgupta@uta.edu. Fax: 817 272-3808.

Present Address

†Y.-H.L.: Department of Chemistry, School of Science, Xi'an Jiaotong University, Xi'an 710049, China.

Notes

The authors declare no competing financial interest.

■ ACKNOWLEDGMENTS

This work was supported by NSF EAGER Grant CHE-1246368. We thank Phillip Shelor for his assistance throughout this work.

■ REFERENCES

(1) Platt, U.; Perner, D.; Patz, H. W. *J. Geophys. Res., C: Oceans Atmos.* **1979**, *84*, 6329−6335.
(2) White, J. U. *J. Opt. Soc. Am.* **1942**, *32*, 285−288.
(3) Herriott, D.; Schulte, H. *Appl. Opt.* **1965**, *4*, 883−891.
(4) Lei, W.; Fujiwara, K.; Fuwa, K. *Anal. Chem.* **1983**, *55*, 951−955.
(5) Fuwa, K.; Lei, W.; Fujiwara, K. *Anal. Chem.* **1984**, *56*, 1640−1644.
(6) Fujiwara, K.; Fuwa, K. *Anal. Chem.* **1985**, *57*, 1013−1016.
(7) Dasgupta, P. K.; Petersen, K. *Spectroscopy* **1987**, *2*, 50−51.
(8) Teshima, N.; Li, J. Z.; Toda, K.; Dasgupta, P. K. *Anal. Chim. Acta* **2005**, *535*, 189−199.
(9) Dress, P.; Franke, H. *Rev. Sci. Instrum.* **1997**, *68*, 2167−2171.
(10) Altkorn, R.; Koev, I.; Van Duyne, R.; Litorja, M. *Appl. Opt.* **1997**, *36*, 8992−8998.
(11) Dallas, T.; Dasgupta, P. K. *Trends Anal. Chem.* **2004**, *23*, 385−392.
(12) Dasgupta, P. K. *Anal. Chem.* **1984**, *56*, 1401−1403.
(13) Robertson, C. W.; Williams, D. *J. Opt. Soc. Am.* **1971**, *61*, 1316−1320.
(14) Wieliczka, D.; Wang, S.; Querry, M. R. *Appl. Opt.* **1989**, *28*, 1714−1719.
(15) Dasgupta, P. K.; Rhee, J. S. *Anal. Chem.* **1987**, *59*, 783−786.
(16) Islam, M.; Seetohul, L. N.; Ali, Z. *Appl. Spectrosc.* **2007**, *61*, 649−658.
(17) Seetohul, L. N.; Ali, Z.; Islam, M. *Anal. Chem.* **2009**, *81*, 4106−4112.
(18) Fielder, S. E.; Hese, A.; Ruth, A. A. *Chem. Phys. Lett.* **2003**, *371*, 284−294.
(19) Fielder, S. E.; Hese, A.; Ruth, A. A. *Rev. Sci. Instrum.* **2005**, *76*, 023107.
(20) O'Keefe, A. *Chem. Phys. Lett.* **1998**, *293*, 331−336.
(21) O'Keefe, A.; Scherer, J. J.; Paul, J. B. *Chem. Phys. Lett.* **1999**, *307*, 343−349.